NREL
NATIONAL RENEWABLE ENERGY LABORATORY

A Flat ATIR Optics Approach to CPV

December 3, 2009 — December 3, 2010

David Schultz
Banyan Energy, Inc.
Berkeley, California

NREL is a national laboratory of the U.S. Department of Energy, Office of Energy Efficiency & Renewable Energy, operated by the Alliance for Sustainable Energy, LLC.

Subcontract Report
NREL/SR-5200-51859
Revised October 2011

Contract No. DE-AC36-08GO28308

NREL
NATIONAL RENEWABLE ENERGY LABORATORY

A Flat ATIR Optics Approach to CPV

December 3, 2009 — December 3, 2010

David Schultz
Banyan Energy, Inc.
Berkeley, California

NREL Technical Monitor: Harin S. Ullal
Prepared under Subcontract No. NEU-0-99010-11

National Renewable Energy Laboratory

1617 Cole Boulevard
Golden, Colorado 80401

303-275-3000 • www.nrel.gov

Subcontract Report
NREL/SR-5200-51859
Revised October 2011

Contract No. DE-AC36-08GO28308

NOTICE

Available electronically at http://www.osti.gov/bridge

Available for a processing fee to U.S. Department of Energy
and its contractors, in paper, from:

U.S. Department of Energy
Office of Scientific and Technical Information
P.O. Box 62
Oak Ridge, TN 37831-0062
phone: 865.576.8401
fax: 865.576.5728
email: mailto:reports@adonis.osti.gov

Available for sale to the public, in paper, from:

U.S. Department of Commerce
National Technical Information Service
5285 Port Royal Road
Springfield, VA 22161
phone: 800.553.6847
fax: 703.605.6900
email: orders@ntis.fedworld.gov
online ordering: http://www.ntis.gov/help/ordermethods.aspx

Cover Photos: (left to right) PIX 16416, PIX 17423, PIX 16560, PIX 17613, PIX 17436, PIX 17721

Printed on paper containing at least 50% wastepaper, including 10% post consumer waste.

Table of Contents

What follows is a chronological summary of technical progress made from December 3, 2009 through December 3, 2010 pertaining to subcontract NEU-0-99010-11.

1 Q1 SUMMARY

1.1 Introduction

An agglomeration of factors has stifled the economic promise of CPV. Foremost among these factors are: insufficient optical efficiency, misfit with existing solar infrastructure and production capabilities, and inadequate reliability of the optic-receiver pairing. These difficulties are largely driven by the choice of optic. The CPV industry is constrained in a paradigm of bulky reflective or refractive optics that operate best at either low concentration (2-5x) or high concentration (100x and above). Low concentration approaches are plagued by marginal economics, while high concentration approaches face heightened technical risks. High concentration systems inevitably face thermal management hurdles and often do not fit well with the existing solar infrastructure. Using Aggregated Total Internal Reflection (ATIR) as the optical mechanism for gathering light, a cost effective, line-focus optic can be produced at scale to provide superior optical efficiency in a flat profile and operate at a mid level of concentration to mitigate the tradeoff between economic benefit and adoptability. Substantiating this motivational premise behind the ATIR optics approach to CPV requires performance data.

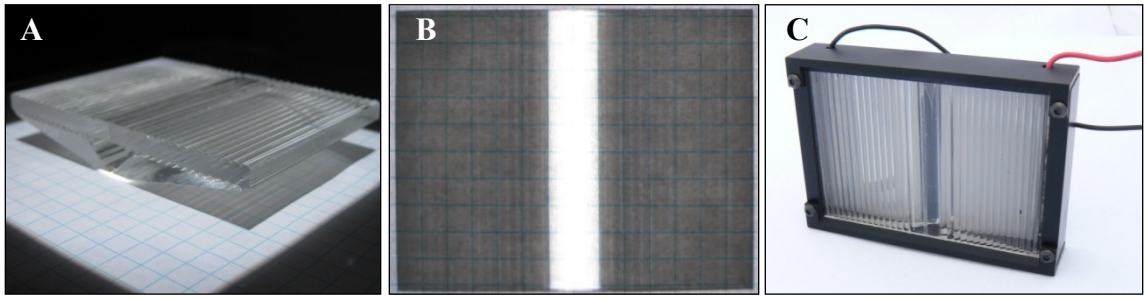

Figure 1. An early ATIR lens prototype (A) that has an aspect ratio of 7:1 and produces a line-focus silhouette (B). A single-unit module prototype demonstrates module integration (C).
Photos from Banyan Energy

Foremost among the goals for establishing the viability of ATIR optics in solar is demonstrating optical efficiency. The first deliverable and milestone defined in the Statement of Work required that Banyan Energy deliver prototype optics and demonstrate an optical efficiency in excess of 78.3%.

Banyan Energy performed an outdoor test of optical efficiency (OE) based on short circuit current using the line-focus Lens Step prototype. Optical efficiency of 84.7% and acceptance angles of ±2.8˚ and ±17.2˚ (acceptance angles about the tracked and non-tracked axes, respectively) were measured. This validates optical modeling efforts which predicted a nominal optical efficiency and acceptance angle about the tracked axis of 84.2% and 3.0˚ respectively. The achieved optical efficiency mark exceeds the threshold value of 78.3% specified for the completion of Milestone #1. Along with the data supporting these measurements, two assembled optics were sent to NREL in fulfillment of the first deliverable for the subcontract.

In addition to achieving the first set of deliverables, Banyan Energy has begun work towards module integration; specifying production processes, demonstrating bonds at all critical interfaces and conducting preliminary reliability tests. Demonstrating a multiunit module construction with reasonable efficiency is our next milestone.

1.2 Methods

The primary technical challenge for Q1 was to formulate a rigorous measurement of optical efficiency. The short circuit current of a solar cell, J_{sc}, is proportional to the amount of incident irradiance. Therefore, optical efficiency can be measured as the resource-adjusted proportion of short circuit current readings from the cell with and without the optic. Measurements were taken outdoors on a custom 2-axis tracker (Small Power Systems Inc., Covelo, CA). A custom silicon solar cell designed to accommodate 8 sun incident power was provided by NaREC and used as the detector. For each measurement a full IV curve was recorded, as well as the Global and Direct Normal Irradiance (GNI and DNI, respectively). The input measurement was taken with the detector cell mask-delimited. The lens step optic is then coupled to the cell with the non-curing silicone elastomer base (Sylgard 184 Base, DOW, Midland, MI) facilitating the output measurement. Optical efficiency is computed as the ratio of input to output measurements after the input measurement has been normalized for the differences in area and solar resource between the two tests:

$$OE = \frac{J_{sc,final}}{J_{sc,initial}} = \frac{J_{sc,2}}{\left(J_{sc,1} * \frac{A_{optic\ input}}{A_{mask}} * \frac{DNI_2}{GNI_1}\right)} = \frac{J_{sc,2}}{J_{sc,1}} * \frac{A_1}{A_{input}} * \frac{GNI_1}{DNI_2}$$

Optical efficiency measurements were complimented by acceptance angle measurements generated by measuring peak power output at varying degrees of tracker misalignment about the axis of the optic.

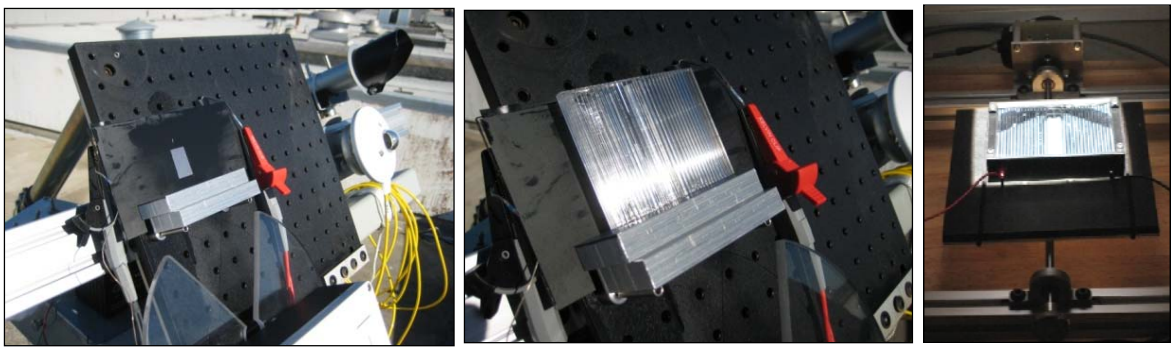

Figure 2. (A) Masked cell baseline testing on custom two-axis tracker (Note: DNI and GNI sensors mounted in background) (B) Lens Step Prototype optically coupled to cell (C) Minimodule mounted on a custom acceptance angle testing platform.
Photo from Banyan Energy

The implemented test method departed from the test method described in the SOW in three areas: 1) A bare reference cell is used instead of a packaged cell due to unexpected optical effects in the extra packaging layers; 2) The test was preformed outdoors under the sun instead of indoors with a solar simulator due to the solar simulator not meeting specifications; 3) The

reference cell used for testing was not sent to NREL for verification of J_{sc} linearity with respect to incident flux because the metallization was designed to be sufficient to insure linearity past our incident flux levels.

In addition to the testing required in the Statement of Work, Banyan Energy conducted experiments to measure the acceptance angle envelope for the Lens Step prototype optic. Acceptance angles were measured at Banyan Energy's indoor testing facility. An acceptance angle profile is generated by first measuring peak power while aligned with the light source followed by power measurements over an array of misaligned orientations. The acceptance angle envelope is defined as the range of primary and secondary axes misalignments over which a solar module achieves greater than 90% of its peak power production.

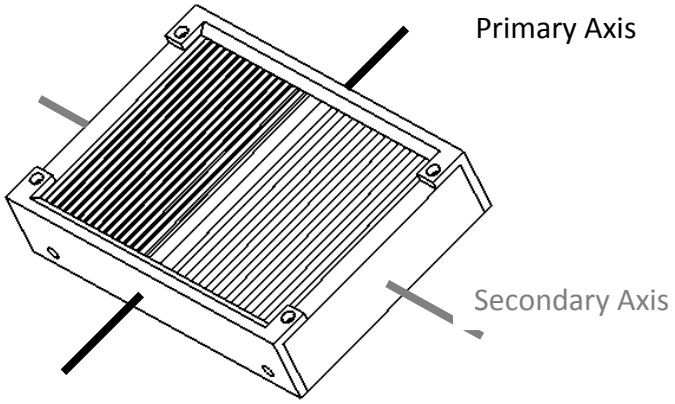

Figure 3. Minimodule prototype primary and secondary axes illustrated.

1.3 Results

As indicated in the introduction, the average optical efficiency measurement was 84.7% with a standard deviation of 1.3%. The relatively small amount of variability was primarily driven by the limitations of the pyranometer used for measuring GNI. Given this variability, the measured value of 84.7% was not significantly different from the predicted value of 84.2%.

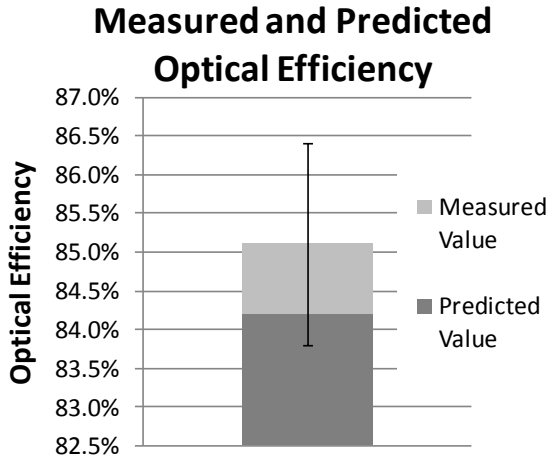

Figure 4: Input measurement with delimited cell mounted on 2 axis tracker. (N=9)

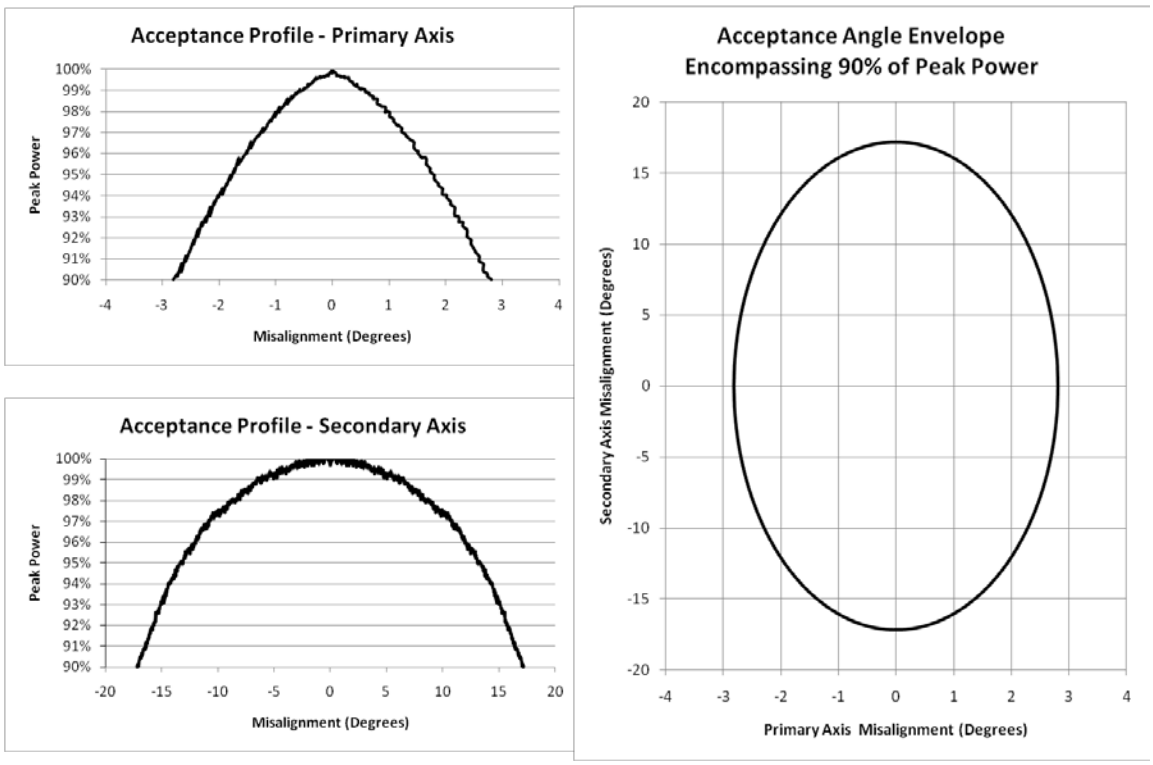

Figure 5. Acceptance angle profiles for the Lens Step primary and secondary axes (Left) and a 2-D minimum volume ellipse that defines the misalignment envelope for achieving greater than 90% P_{max} (Right).

Primary axis acceptance angles and secondary axis acceptance angles had ranges of ±2.8˚ and ±17.2˚, respectively. The resolution of these measurements was within 0.17˚ limited primarily by the resolution of the angle encoders used to gauge the orientation of the test platform.

1.4 Discussion

The results of these tests indicate industry leading optical efficiency and wide acceptance angles. This proves the performance of the Banyan Energy ATIR concept and validates the modeling approach. An optical efficiency of 84.7% is competitive with the optical efficiencies offered by competing optical systems, such as Fresnel lenses or reflective troughs. Next generation optics promise improved optical performance that may enable optical efficiency closer to 90%. Acceptance angles beyond ±2˚ are sufficient to accommodate tracking imprecision, structural imprecision and capture circumsolar radiation. The Lens Step optic provides an envelope that goes beyond this minimum and secondary axis acceptance angles on the order of ±20˚ enable more tracking options. Next generation designs also promise improvements with respect to acceptance angles. These results not only fulfill initial tasks outlined in the Statement of Work, but enable a viable product and further motivate the module integration work underway.

2 Q2 SUMMARY

2.1 Introduction

Technical progress in Q2 focused on module design and integration of optics into a working prototype. Task 2 outlined in the Statement of Work called for Banyan Energy to integrate Gen 1 optics produced and tested during Task 1 into several multi-unit modules suitable for on-sun testing.

In Banyan Energy's Q1 report, optical efficiency (OE) was calculated based on short circuit current (J_{sc}) because short circuit current tends to be insensitive to temperature changes and proportional to radiant energy flux. It was necessary to normalize current readings by the proportion of cell area (A_1) and optic area (A_2) and normalize for differences in radiant energy resource. The bare cell garners both direct and diffuse light resource which can be cumulatively measured via a Global Normal Irradiance (GNI) reading from a pyranometer. The concentrator unit (cell + optic) is expected to capture primarily direct light which can be measured with a Direct Normal Incidence (DNI) reading from a pyrheliometer. Optical efficiency was calculated as follows:

$$OE = \frac{J_{sc,final}}{J_{sc,initial}} = \frac{J_{sc,2}}{J_{sc,1}} * \frac{A_1}{A_2} * \frac{GNI_1}{DNI_2} \qquad (1)$$

The threshold module performance for the fullfillment of Task 2 was based on this equation and short circuit current readings) with some modifications. First, optical efficiency was fixed at Banyan Energy's target value of 90%. Second, a module integration loss factor of 0.7 was applied in order to give sufficient error budget for potential integration losses. The module output current was required to be greater than the product of the normalized baseline cell current, optical efficiency and the integration loss factor. Expressed more concisely:

$$J_{sc,2} > 0.7(OE)\ (J_{sc,1} * \frac{A_2}{A_1} * \frac{DNI_2}{GNI_1}) \qquad (2)$$

2.2 Methods

In order to establish baseline peformance without the optic, short circuit current ($J_{sc,1}$) was measured for a series of four cells attached to a corrugated backplane; the relevant resource basis for these readings was GNI. The backplane was fitted with dielectric in order to insulate electrically active connections. Cells were wired in serries, fixed in location and laminated to the backplane. Black electrical tape was temperarily affixed over the laminant material to the non-cell areas in order to minimize the effect of light being reflected from the corrugated backplane to the cell. The backplane assembly was then mounted normal to the sun on a two axis tracker (Figure 1). Throughout testing, tracking precision was verified to be within ±0.25˚ via a visual alignment indicator consisting of a mirror coupled to an offset aperture. A series of ten I-V readings were taken reccording: short circuit current (J_{sc}), open circuit voltage (V_{oc}), maximum power (P_{max}), fill factor (FF), conversion efficiency, direct normal irradiance (DNI) and global normal irradiance (GNI). The electrical tape was then removed, optics were coupled to the cells using a silicone elastomer, a frame was affixed, the module was mounted on the tracker and a new serries of ten electrical peformance readings was taken; the relevant resource basis for these readings was DNI. Due to assembly time, the second set of readings was often taken at a later

date. By pairing simultaneous resource data with electrical peformance data it was possible to normalize based on resource, mitigating the effect of differing test times and changing resource conditions.

Figure 1. Milestone 2 outdoor test photos from baseline test and module test. Baseline test with cells mounted on a corrugated backplane (left). Note: the aluminum was masked with electrical tape to minimize reflection from the angled facets of the backplane. The same backplane (electrical tape removed) with optics mounted on the cells and frame attached (right). Resource sensors, including a pyranometer, pyrheliometer and a reference cell are mounted in the background. Visual alignment indicator and tracker controller are mounted in the foreground. ***Photos from Banyan Energy***

The ratio of active cell area to effective optic apperture area can be calculated with reference to the module geometry denoted in Figure 3 as follows:

$$A_2 = 4 * x_2 * y_1$$
$$A_1 = 4 * x_1 * y_1$$
$$\frac{A_2}{A_1} = \frac{x_2}{x_1}$$

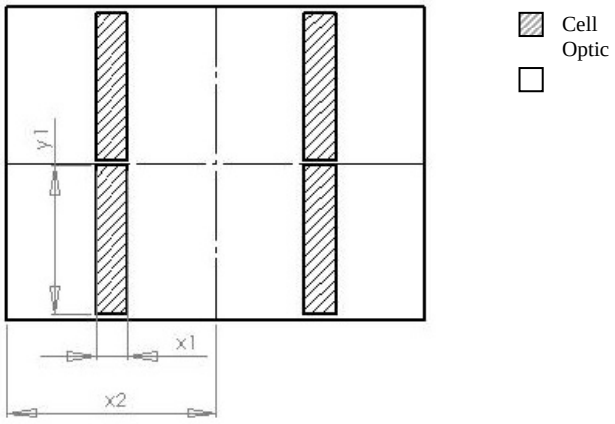

Figure 2. Schematic of a four-unit module showing the dimensions used to calculate the ratio of active cell area and effective optic aperture area. x1 is equivalent to the active width of the cell, y1 is equivalent to cell length and x2 is equivalent to the width of the optic.

The relevant area ratio (A_2/A_1) is equivalent to the ratio of average optic width (x_2 = 89.0mm) to average cell active area width (x_1 =13.4mm). Reducing equation 2 by substituting known constants (module integration loss factor, optical efficiency and area ratio) provides a simple expression to evaluate performance relative to the threshold defined for Milestone 2:

$$J_{sc,2} > 4.18\ (J_{sc,1} * \frac{DNI_2}{GNI_1}) \qquad (3)$$

2.3 Results

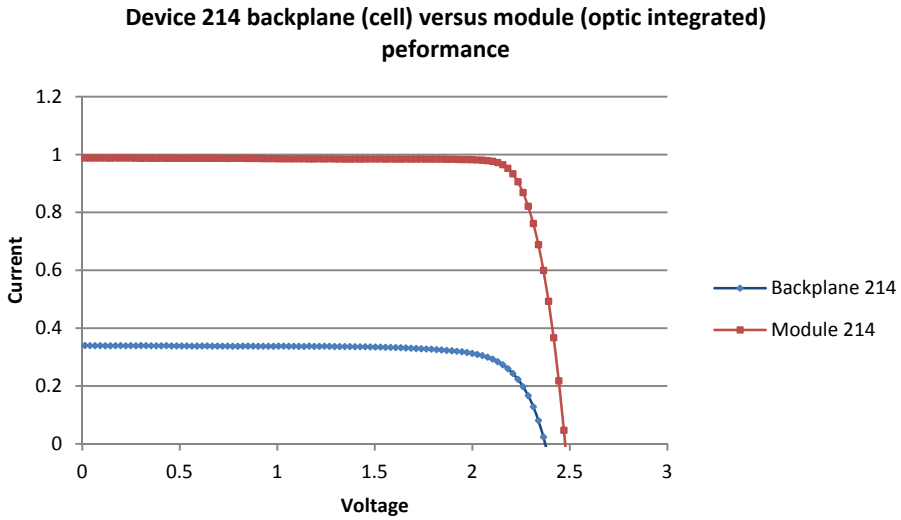

Figure 3. Device 214 I-V curves before and after prototype optic integration.

Table 1. Device 214 representative electrical performance data before and after prototype optic integration (corresponds to I-V curves shown in Figure 4).[1]

DUT	Pmax	Imp	Vmp	Isc	Voc	FF	Eff	AVG_DNI	AVG_GNI
Backplane 214	0.609	0.301	2.025	**0.324**	2.374	0.791	15.5	806.1	**1069.1**
Module 214	2.432	1.171	2.078	**1.224**	2.471	0.804	12.1	**855.3**	1067.4

Representative V-I readings indicate a baseline short circuit current of 0.324 Amperes with a global normal irradiance of 1069 W/m^2 (Table 1). With the optics integrated, the short circuit current exceeded 1.22 Amperes under a direct normal irradiance of 855 W/m^2 (Figure 3, Table 1). These representative numbers indicate that the output short circuit current exceeded the threshold value of 1.08A (Equation 3) by 12.9%. The performance threshold was exceeded for all 10 measurements in the test series.[2] The full dataset supporting this claim is provided as an addendum file.

[1] Data has the following corresponding units: W, A, V, A, V, %, %, W/m^2, W/m^2 – for each of the respective columns in Table 1.
[2] The full datasets for each of the two modules delivered are provided in separate files.

2.4 Discussion

Results indicated that the module electrical performance exceeded the threshold defined in the SOW in all cases. The Gen 1 prototype optics continue to perform well and can be readily assembled into a module. ATIR optics can be integrated into a flat module form factor and mated with cells to produce energy. With low volume assembly methods, module integration losses were observed as expected. For example, cells for Module 214 were individually measured to be between 16.0-16.3% efficient, however, when laminated in series on the aluminum backplane, the module-integrated string efficiency decreased to 15.5%. Imperfections in solder joints and series resistance likely decreased receiver performance. Previously, the Gen 1 prototype optic was measured to be approximately 84%. Given this optical efficiency, the maximum achievable efficiency on a 15.5% efficient receiver is 13.0%. Module 214 achieved 12.1% efficiency. This 0.9% absolute efficiency loss was, at least in part, due to variability in optic performance. Currently, prototype optics consist of individual tiles that each have a set of imperfections that decrement optical efficiency. Optical losses are also likely to increase due to imperfections in the encapsulant layer. Just as cells in series are current limited by the lowest performing cell, so too are concentrator units in series limited by the lowest performing optic-cell pair.

During module assembly, process control is paramount. A redesign effort is underway focused on design for manufacturing and design for assembly in order to minimize cost and improve reliability.

Figure 4. Left: multi-unit module. Right: modules on sun. ***Photos from Banyan Energy***

3 Q3 SUMMARY

3.1 Introduction

Technical progress in Q3 focused on module design and integration of production optics into a working prototype. Banyan Energy is currently in the process of acquiring prototype parts and working through low scale assembly methods. Task 3 outlined in the Statement of Work called for Banyan Energy to design and integrate production optics into a multi-unit module for test.

Recall that in Q2 of the program optical efficiency (OE) was determined based on short circuit current (J_{sc}) because short circuit current tends to be insensitive to temperature changes and proportional to radiant energy flux. Accordingly, the threshold module performance for the fullfillment of Task 2 defined in the SOW was based on the following equation:

$$J_{sc,2} > 0.70(OE)\left(J_{sc,1} * \frac{A_2}{A_1} * \frac{DNI_2}{GNI_1}\right) \qquad (1)$$

Where J_{sc} is the short circuit current, A is the active aperture, DNI is the direct normal irradiance and GNI is the global normal irradiance. The subscripts 1 and 2 indicate pre-optic and post-optic configurations, respectively. In this threshold relationship for Task 2, optical efficiency (OE) was fixed at Banyan Energy's target value of 90% and a module integration loss factor of 0.70 was applied in order to give sufficient error budget for potential integration losses. For the fullfillment of Task 3 the peformance metric is much the same as that for Task 2; the difference being that the module integration loss factor is less lenient having a value of 0.85.

$$J_{sc,2} > 0.85(OE)\left(J_{sc,1} * \frac{A_2}{A_1} * \frac{DNI_2}{GNI_1}\right) \qquad (2)$$

Banyan Energy continues to work towards exceeding this threshold for short circuit current. However, there exist some notable differences between design intent indicated in the SOW and current design hypotheses. The initial intent stated in the SOW for the new optic was to concurrently increase the acceptance angle profile beyond ±3˚, increase the geometric concentration towards 10x while maintaining a high optical efficiency (targeting 90%) and reducing part count to improve manufacturing economics. Since formulating the SOW, we have refined our design process; particularly with respect to selecting an appropriate acceptance angle and level of concentration. What follows is a rationale behind revising optic design parameters from what was indicated in the SOW.

For non-imaging optics there exists a fundamental tradeoff between acceptance angle and the level of concentration. As the level of concentration increases, the acceptance angle tends to be more constrained and vice-versa. Over-sizing the acceptance angle budget for misalignments stemming from module assembly, mounting assembly, tracker precision and ground settling will result in undue constraint on the level of concentration and aspect ratio. In other terms, considering optic design parameters are dependent, there is no incentive to make the acceptance angles larger than necessary. Rather, acceptance angle budget needs to be rigorously vetted and then used as a fixed design parameter. Our initial acceptance angle target of ±3˚ (calculated at 90% of peak power) is sufficient to accommodate the aforementioned sources of misalignment

and has marketplace validation[3]. Therefore this value was not changed in the current design effort. Furthermore, although the optic design has changed substantially from the first generation design, the target level of geometric concentration remains in the 7-8x range. The reason for this target is that our estimates indicate that a 5-10x effective flux increase is an optimal range for an LCPV product considering the technical and economic tradeoffs that follow from the level of concentration selected. After an optical efficiency of 80-90% is taken into account, a 7-8x geometric optical design outputs roughly 5-7x effective flux. We briefly explain the rationale behind the target range for concentration as follows:

There are 5 essential relationships that affect a CPV product based on the level of concentration. They are: cell cost per unit area (i.e. the capital efficiency benefit), cell efficiency, cell operating temperature (which ultimately impacts cell efficiency and reliability), acceptance angle, and manufacturing feasibility (Figure 1). Cell cost reduces non-linearly with increasing concentration such that there are diminishing marginal returns. Certain cell architectures show efficiency increases under concentration on the order of 10%. For the current Banyan Module architecture this benefit has a broad peak in a range of 5-10x effective concentration (Figure 2). Concurrent with this efficiency benefit, cell efficiency tends to decrease with increasing concentration due to the temperature effect on output voltage. And module life will decrease with more intense thermal cycling associated with higher levels of concentration. This assumes that higher concentration designs cause higher nominal operating cell temperatures. As was mentioned previously, increasing the level of concentration tends to narrow the acceptance angle profile, which must remain above the tracking error budget. Finally, increasing concentration tends to require reduced manufacturing tolerances that in turn increase cost or make the optic infeasible altogether. For example, increasing the level of concentration from 7x to 12x within a module form factor adds a modest capital efficiency benefit, but begins to constrain performance and life expectancy due to more intense thermal load. Perhaps even more critical to note in this scenario is the simple observation that cell sizes begin to get quite small (on the order of a few millimeters). At some point, handling small cells in a manufacturing process becomes too costly, especially as yields diminish. The feedback we have received from contract manufactures and experts who know cell handing equipment is that cell width should target the 10mm range in order to avoid yield loss and radical tooling changes. This example highlights the tradeoffs that dictate the appropriate level of concentration for a given receiver type.

[3] Confidential discussions with two vertically integrated silicon PV companies who have an interest in our product and also produce trackers have verified assumptions regarding viability of a ±3˚ acceptance angle design.

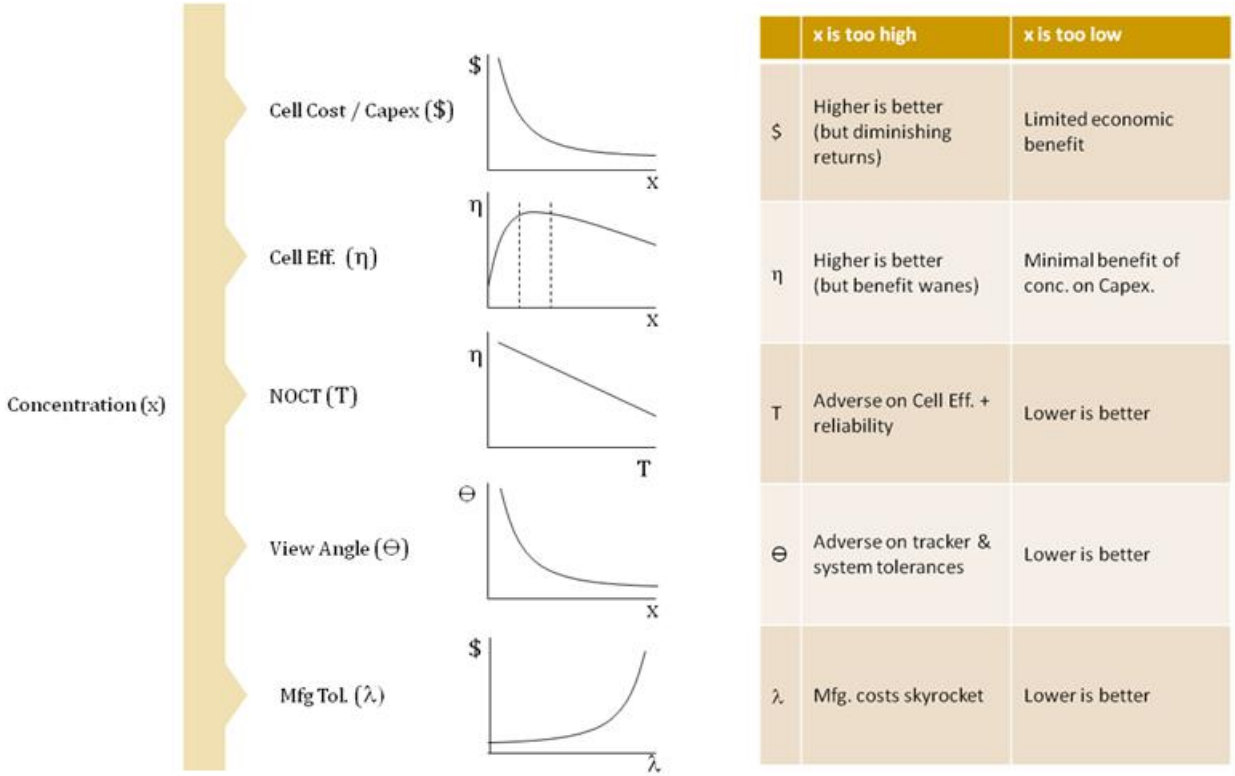

	x is too high	x is too low
$	Higher is better (but diminishing returns)	Limited economic benefit
η	Higher is better (but benefit wanes)	Minimal benefit of conc. on Capex.
T	Adverse on Cell Eff. + reliability	Lower is better
Θ	Adverse on tracker & system tolerances	Lower is better
λ	Mfg. costs skyrocket	Lower is better

Figure 6. Five notable tradeoffs stemming from the level of concentration selected for a CPV design.

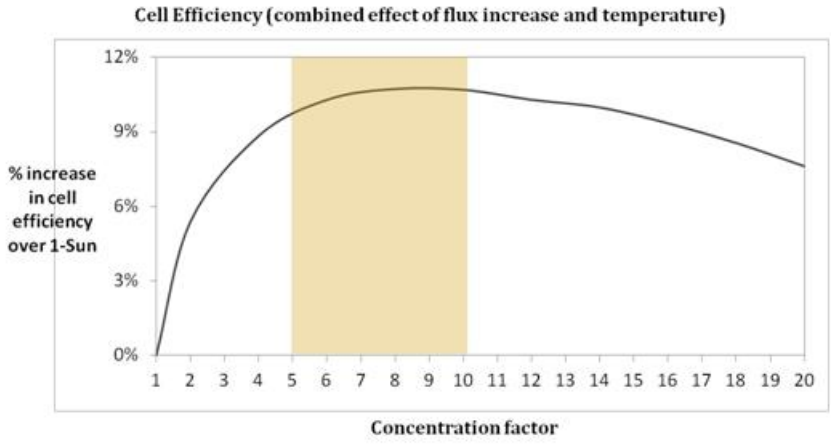

Figure 7. Cell efficiency profile with increasing concentration. Note that this empirical data takes into account the effect of increasing temperatures at increased levels of concentration for the first generation Banyan module architecture. The shaded region indicates the broad peak that defines an optimal operating range.

Having proven manufacturability for a certain characteristic feature size in the first generation optic and verified cost models with potential customers, four main factors have driven us to design for a level of concentration in the 7-8x range rather than increasing the concentration to the 10x target put forth in the SOW. Namely, maintaining acceptance angles, maintaining cell width, minimizing thermal load (without having to add fins) and maximizing cell efficiency.

3.2 Optical Design Overview

The evolution of the production optic design from the current prototype design can be summarized as follows: The concentrating and redirecting functionality of the prototype primary optic have been integrated into the cover glass and waveguide optic, respectively; thus, eliminating the need for a concerted primary optic altogether. Waveguide parts have been lengthened by a factor of 3 to reduce part count and improve throughput. Total optic part count has been reduced by a factor of 6 for each square meter of module. The optic parts have been made simpler, with fewer, large features; this reduces the need for tight tolerances and allows for performance stability with thermal cycling.

3.3 Project Status

Prototype parts for the production module have been ordered and are expected by mid-August 2010. Assembly and testing are expected to commence in August with refinements to follow. Given the progress thus far, it is anticipated that the deliverables for Task 3 can be achieved within the allotted time; the deadline being December 3, 2010.

4 Q4 SUMMARY

4.1 Introduction

Technical progress in Q3 and Q4 focused on module design and integration of production optics into a working prototype. Task 3 outlined in the Statement of Work called for Banyan Energy to design and integrate production optics into a multi-cell prototype module for testing. Banyan Energy has now produced several 4-cell prototypes that demonstrate the performance and the module integration of the next generation of optics. The new optic design shows improvements in optical efficiency and acceptance angle profile, but perhaps more crucial to the long term success of the product is that it reduces manufacturing costs by relaxing tolerances and requiring fewer parts. Also notice that the backplane is now flat, as opposed to the previous design that was corrugated. This design change allows the receiver package to be produced with conventional lamination process.

In Banyan Energy's Q1 report, optical efficiency (OE) was calculated based on short circuit current (J_{sc}) because short circuit current tends to be insensitive to temperature changes and proportional to radiant energy flux. It was necessary to normalize current readings by the proportion of active cell area (A_1) and optic area (A_2) as well as normalize for differences in radiant energy resource. The bare cell garners both direct and diffuse light resource which can be cumulatively measured in Watts per square meter via a Global Normal Irradiance (GNI) reading from a pyranometer (CMP-3, Kipp & Zonen, Netherlands). The concentrator unit (cell + optic) is expected to capture primarily direct light which can be measured with a Direct Normal Incidence (DNI) reading from a pyrheliometer (CHP-1, Kipp & Zonen, Netherlands). Optical efficiency was calculated as follows:

$$OE = \frac{J_{sc,final}}{J_{sc,initial}} = \frac{J_{sc,2}}{J_{sc,1}} * \frac{A_1}{A_2} * \frac{GNI_1}{DNI_2} \qquad (1)$$

The threshold module performance for the fullfillment of Task 3 was based on this equation and short circuit current readings with some modifications. First, optical efficiency was fixed at Banyan Energy's target value of 90%. Second, a module integration loss factor of 0.85 was applied in order to give sufficient error budget for potential integration losses. Recall that in Task 2 the module integration factor was less stringent at 0.70. The module output current was required to be greater than the product of the normalized baseline cell current, optical efficiency and the integration loss factor. Expressed more concisely:

$$J_{sc,2} > 0.85(OE)\ (J_{sc,1} * \frac{A_2}{A_1} * \frac{DNI_2}{GNI_1}) \qquad (2)$$

The relevant area ratio (A_2/A_1) is equivalent to the ratio of the active module aperture area (not including support rib area) to the active cell area. Subscripts 1 and 2 imply pre-optic (receiver only) and post-optic assemblies, respctively. In addition to validating electrical performance according to this threshold, the acceptance angle profile for the new optic was measured and reported.

4.2 Methods

In order to establish baseline peformance without the optic, short circuit current ($J_{sc,1}$) was measured for a series of four cells attached to a backplane along with the relevant resource basis for these readings, GNI. The backplane was fitted with dielectric in order to insulate electrically active connections. Cells were wired in series and laminated to the backplane. The backplane assembly was then mounted normal to the sun on a two axis tracker. Throughout testing, tracking precision was verified to be within ±0.25˚ via a visual alignment indicator consisting of a mirror coupled to an offset aperture. A series of current-voltage sweeps were taken recording: short circuit current (J_{sc}), open circuit voltage (V_{oc}), maximum power (P_{max}), fill factor (FF) and conversion efficiency. Also recorded for each sweep were direct normal irradiance (DNI) and global normal irradiance (GNI). After baseline cell performance was measured, optics were coupled to the cells using a silicone elastomer, a frame was affixed, the module was mounted on the tracker and a new series of electrical peformance readings were taken; the relevant resource basis for these readings was DNI. By pairing simultaneous resource data with electrical peformance data it was possible to normalize power output based on resource, mitigating the effect of differing test times and changing resource conditions.

In addition to the testing required in the Statement of Work, Banyan Energy conducted experiments to measure the acceptance angle envelope for the new prototype optic. An acceptance angle profile is generated by first measuring peak power while aligned with the light source followed by power measurements over an array of misaligned orientations. Acceptance angle profiles were generated about both the primary (daily) axis of rotation and the secondary (seasonal) axis of rotation. By convention, the acceptance angle envelope is defined as the range of primary and secondary axes misalignments over which a solar module achieves greater than 90% of its peak power production.

For the acceptance angle tests, the orientation of the test platform was determined via a ball bearing optical shaft encoder (H6-2500-I-S, US Digital, Vancouver, WA) mechanically coupled to the solar tracker. The encoder had a resolution of 0.14˚. Initial alignment of the test platform was determined via a custom built visual alignment indicator consisting of a 1 mm pin hole aperture spaced 170 mm from a mirror mounted coplanar to the test platform. Visual alignment was established when the aperture and the divergent reflected light from the sun formed concentric circles. The resolution of the visual alignment indicator was 0.17˚. After testing, an error check was performed to validate that peak power production occurred at the initial reading, where visual alignment was achieved. Once initial visual alignment was established the encoder readings were tared and the test platform was allowed to travel through a range of misaligned orientations about each axis while concurrent power measurements were taken.

4.3 Results

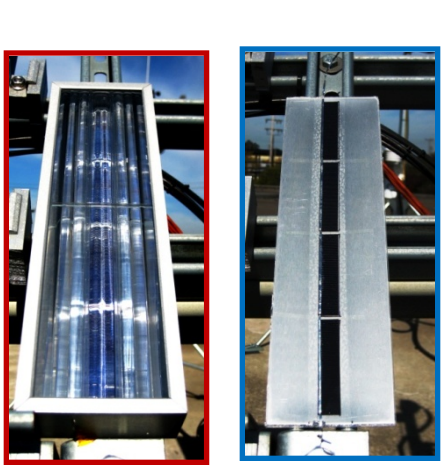

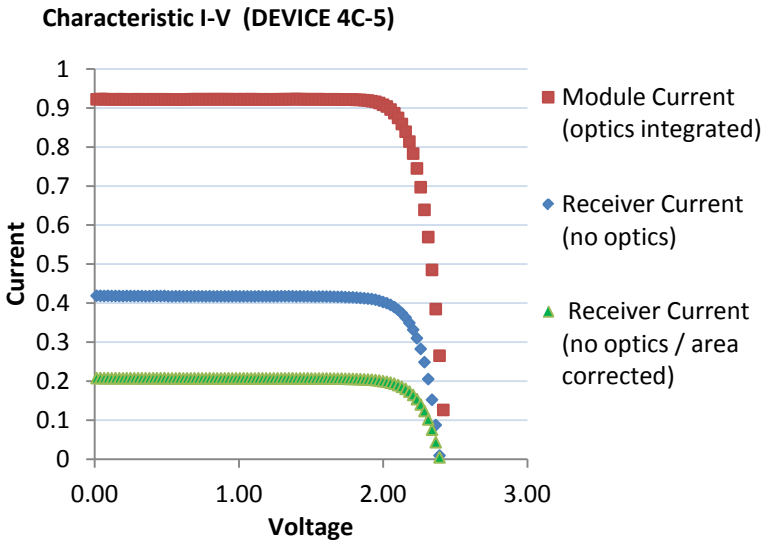

Figure 1. I-V curves before and after prototype optic integration for device 4C-5 are shown in blue and red respectively. Note: cells oversized to ensure overlap. *Photos from Banyan Energy*

Cells were oversized in the width dimension by approximately 100% (cell width = 19mm, focal area width = 9.4mm) in order to allow for substantial misalignment error during manual assembly. Also, Banyan Energy wanted to minimize costs and use up an inventory of pre-diced cells from previous prototypes. The area-corrected characteristic I-V curve can be calculated by simply scaling the receiver data by the area ratio (Figure 1). This area-corrected data represents achievable performance once process controls are in place to precisely match and register the cell dimensions and location with the optic focal area. Note that although these results show a 2.3x power amplification once the receiver is paired with the optic (Table 1), a 4.7x power amplification is expected for this particular prototype if cell size and position are properly matched with focal area.

Table 1. Parameters from the test (corresponds to I-V curves shown in Figure 2).[4] Parameters in bold were used to verify performance exceeded the threshold. Aperture areas for the receiver and module were 4750 and 16896 mm^2 respectively.

DUT	P_{max}	I_{mp}	V_{mp}	J_{sc}	V_{oc}	FF	Eff	AVG_DNI	AVG_GNI
Receiver 4C-5	0.8046	0.3922	2.051	**0.419**	2.375	80.7	16.04	918	**1056**
Module 4C-5	1.8410	0.8862	2.078	**0.923**	2.437	81.7	13.50	**807**	1026

Characteristic I-V readings indicate a receiver short circuit current ($J_{sc,1}$) of 0.419 Amperes under an average global normal irradiance (GNI_1) of 1056 W/m^2 (Table 1). With the optics integrated, the short circuit current ($J_{sc,2}$) exceeded 0.923 Amperes under a direct normal

[4] Data has the following corresponding units: W, A, V, A, V, %, %, W/m^2, W/m^2 – for each of the respective columns in Table 1. Note that receiver and module efficiencies are measured on GNI and DNI bases respectively.

irradiance (DNI_2) of 807 W/m^2 (Figure 2, Table 1). These representative numbers indicate that the output short circuit current exceeds the threshold value of 0.878 Amps (Equation 3) by 5.14%. The performance threshold was exceeded for all measurements in the test series.[5] The full datasets supporting this claim is provided as an addendum file.

Acceptance angles for the first series of production prototypes were comparable to the first generation of prototypes having primary and secondary acceptance angles of approximately ±3˚ and ±18˚ at 90% of peak power, respectively.

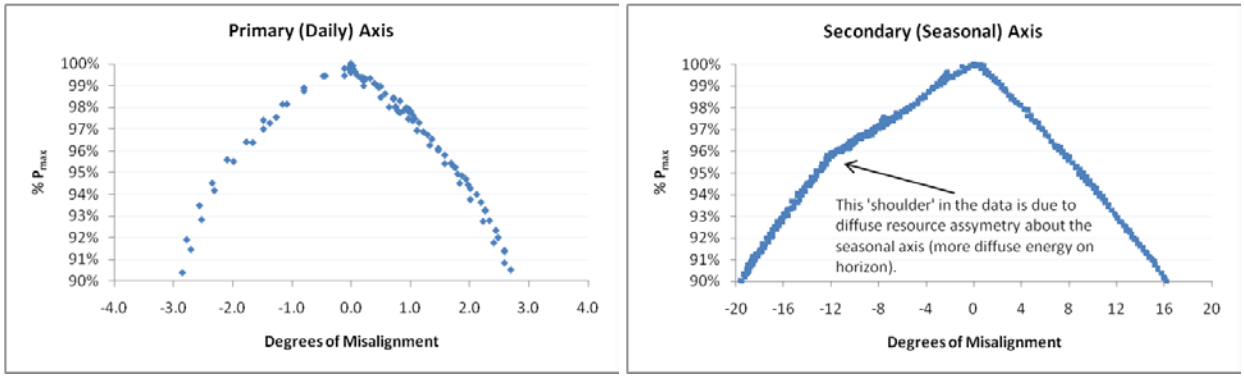

Figure 2. Primary and secondary axis acceptance angle profiles for the first series of production prototypes (specifically 4C-5 here) indicate adequate acceptance angles of approximately ±3˚ and ±18˚ degrees of allowable misalignment at 90% of peak power. Secondary axis data has been cosine corrected to account for the change in projected area.

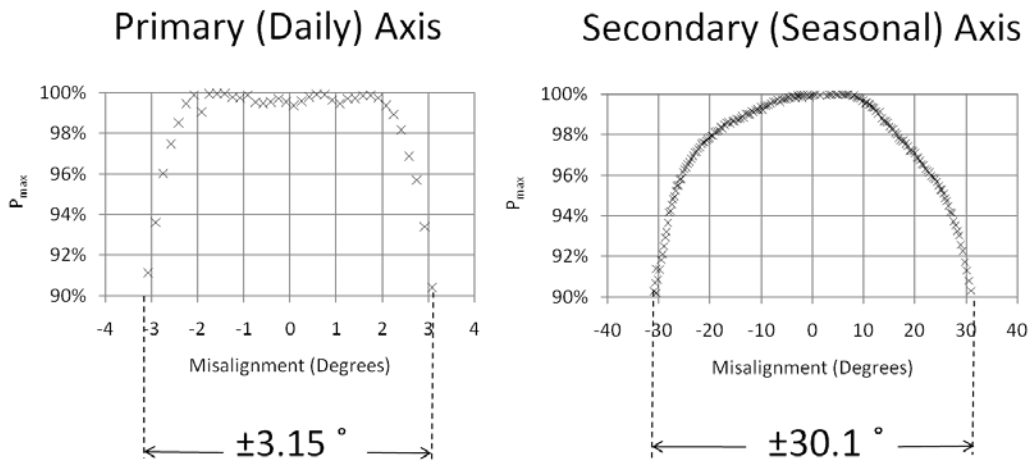

Figure 3. Primary and secondary axis acceptance angle profiles for a refined first generation arrayed module indicate what is achievable for ATIR optic acceptance angle profiles once quality parts and assembly processes are implemented. Note: Data taken from an arrayed (36 cell) gen 1 module (Ulysses) in outdoor 1-sun conditions. The test module achieved an absolute peak power (P_{max}) of 23.4 W during these tests. Secondary axis data has been cosine corrected to account for the change in projected area.

[5] Datasets for each of the two modules delivered are provided in separate files e-mailed to Harin Ullal

4.4 Discussion

Results indicated that the module electrical performance exceeded the threshold defined in the SOW in all cases. Beyond the pre-incubator goals of validating performance possibilities for solar modules with ATIR optics, Banyan Energy is particularly excited about these performance results because the projected costs of parts and assembly at scale for this particular prototype design fit with a profitable economic model. Banyan has worked closely with glass, cell and injection molding suppliers to verify part costs at scale. Further, there exist many opportunities to advance the performance of this particular design. For instance, geometric precision of optic parts at scale will be improved with roll-patterned glass parts and molded parts made with hard tooling rather than aluminum molds. Also, in the final product, antireflective coatings will be applied to the primary optic, increasing optical efficiency considerably. Moving to a back-contact cell in the receiver package will bolster overall power output and may prove to be a more reliable construction. Banyan Energy is currently working on these improvements and a larger (0.25 m^2) version of the production prototype detailed in this report. Current results indicate a 4.7x power amplification for an optic with 7x geometric concentration. The final construction will achieve a power amplification of well over 5x for the same geometric concentration.

Recall that the first generation prototype had acceptance angles at the 90% power point of ±2.8˚ and ± 17.8˚ (about primary and secondary axes, respectively). After improving optic quality in a subsequent series of prototypes these acceptance angles were widened considerably to ±3.1˚ and ±30.1˚. Also, both primary and secondary acceptance angle profiles changed to have more of a flat-top producing near 100% of peak power from a range of ±2˚ and ±20˚ (Figure 3). For this first production prototype we achieved acceptance angles of approximately ±3˚ and ± 18˚, comparable or slightly better than what was achieved for the first series of prototypes (Figure 2). Given the early stage of development for the new production optic, there is reason to believe that these profiles will also see improvements similar to the initial optic.

The pre-incubator program has provided essential technical and financial support. Working with NREL has also provided intangible benefits such as the legitimacy that comes with diligent oversight from experts. The funding management, testing prowess, expertise and oversight of the NREL personnel were essential to building the world's first solar module with ATIR optics. Banyan Energy offers our sincerest thanks for NREL's diligence and help in seeing our early-stage company successfully achieve all three Milestones negotiated in the Pre-Incubator program.

Particular personnel of note on this particular project were Dr. Harin Ullal who helped to negotiate appropriate milestones and shepherd the project to completion within budget and on time. Dr. Keith Emery was also helpful providing testing expertise and recommendations for setting quantifiable goals. Dr. Sarah Kurtz shared her knowledge of the greater CPV industry. Daryl Myers helped in acquiring and understanding solar data; this was essential to Banyan Energy's energy production model. Matt Muller was and continues to be crucial in on-going efforts to test our initial series of quarter-panel prototypes. Banyan Energy would also like to thank all those administrators at NREL and the DOE that help small companies like Banyan begin development of renewable energy technologies in the U.S through the Pre-incubator Program.